EXPERIMENATL INVESTIGATION OF A SUBCOOLED BOILING IN ONE SIDE OF A HEATED RECTANGULAR CHANNEL

Byong Jo Yun, Dong Jin Euh, Chul Hwa Song

Thermal Hydraulics and Safety Research Div., Korea Atomic Energy Research Institute, Korea

Abstract

Downcomer boiling phenomena in a conventional pressurized water reactor have an important effect on the transient behavior of a postulated large-break LOCA (LBLOCA), because it can degrade the hydraulic head of the coolant in the downcomer and consequently affect the reflood flow rate for a core cooling. To investigate the thermal hydraulic behavior in the downcomer region, a test program for a downcomer boiling is being progressed during the reflood phase of a postulated LBLOCA. For this, the test facility was designed as a one side heated rectangular test section which adopts a full-pressure, full-height, and full-size downcomer-gap approach, but with the circumferential length reduced 47.08-fold. The test was performed by dividing it into two-phases: (I) visual observation and acquisition of the global two-phase flow parameters and (II) measurement of the local two-phase flow parameters on the measuring planes along five elevations. In the present paper, the test results of Phase-I and parts of Phase-II are introduced.

Introduction

The APR1400 (advanced power reactor) is an advanced Korean pressurized water reactor that has a rated thermal power of 4000 MW and a 2×4 loop arrangement for the reactor coolant system. It is planned for a commercial operation by 2012, and it adopts new safety injection features such as four mechanically independent safety injection systems, a DVI (direct vessel injection) system that injects the ECC (emergency core cooling) water directly into the reactor vessel downcomer instead of into the cold-leg pipes, fluidic devices in each SIT (safety injection tank) to optimize the ECC flow delivery during a postulated LOCA (loss of coolant accident), an in-containment refueling water storage tank with a steam sparger to reduce the hydrodynamic load to the structure by enhancing the efficiency of a steam condensation, and an elimination of the low-pressure safety injection system [1].

While it is expected that these improvements will greatly enhance the reliability of the ECC system and also reduce the construction costs of the APR1400, some technical issues are addressed because the ECC is injected at a different location than in the previous reactors. That is, the four DVI nozzles are located 2.108 m above the center line of the cold leg, and thus the steam and the injected ECC water are expected to interact in the upper annulus downcomer during the reflood phase of a large-break LOCA (LBLOCA). Fig.1 describes the thermal hydraulics phenomena in the reflood phase

of a LBLOCA in the APR1400. The interactions between the steam and water phases in the upper annulus downcomer may affect the penetration of the ECC water into the core. It is therefore a requisite to evaluate the existing safety analysis codes against the ECC penetration phenomena in the upper annulus downcomer during a postulated LBLOCA of the APR1400. Since there is no available experimental data directly related to the phasic interactions in the upper annulus downcomer, separate effect-test programs including DIVA (DVI visualization and analysis) and MIDAS (multidimensional investigation in downcomer annulus simulation) were progressed by KAERI (Korea Atomic Energy Research Institute) for the ECC bypass phenomena in the upper annulus downcomer [2,3,4].

According to the safety analysis performed for the entire period of a LBLOCA, RELAP5 showed that the downcomer boiling phenomena (which was not accurately simulated in both the DIVA and MIDAS tests) significantly affects the core reflood flow rate [5]. In contrast, this was not observed in the TRAC-M results. This difference between the simulations was mainly attributable to the use of different thermal hydraulics models for the downcomer, especially in the interfacial friction models: RELAP5 uses an interfacial friction model based on the drift flux, whereas TRAC-M uses a modified Blasius friction correlation [6,7]. Different trends were also found for the void fraction and the hydraulic head reduction in the downcomer.

The downcomer boiling phenomena was not an important issue in previous cold-leg injection systems, and thus there have been very few studies on a downcomer boiling. Sudo(1982) performed a separate effect test for the downcomer boiling phenomena which is available in the open literature. The test was performed by using a slab geometry, in which the channel gap and height were 0.2 and 6.5 m, respectively. The test was performed in a transient condition, and it showed the possibility of a degradation of the hydrostatic head due to a downcomer boiling. However, the downcomer gap of the test facility was smaller and its wall was thinner than those of the APR1400, and thus it is difficult to directly extrapolate the test results to the APR1400. In addition, local two-phase flow parameters such as the local void fraction and the interfacial friction factor, which provide information on the internal flow structure, were not measured in the test. The difficulty of separately evaluating the thermal hydraulic models related to a downcomer boiling and developing the relevant physical models resulted in a separate effect-test program for a downcomer boiling being launched at KAERI.

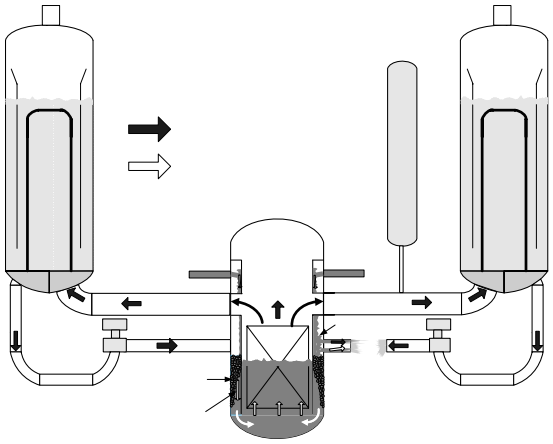

Fig. 1. Major thermal hydraulic phenomena in the primarily system of the APR1400 under the LBLOCA reflood phase.

The goals of the KAERI tests are to produce experimental data (including the local internal flow structure) for use in the evaluation and development of the related thermal-hydraulic models of the computer codes. The test program is being performed by using a two-stage approach: (I) visual observation and acquisition of the global two-phase flow parameters; and (II) measurement of the distribution of the local two-phase flow parameters. The DOBO (**DO**wncomer **BO**iling) test facility, which has a rectangular test section, was set up for the above purposes, and Phase-I and some parts of the Phase-II tests were performed during the postulated reflood phase of a LBLOCA in the present study [10].

Experimental Facility

The DOBO test facility is designed to simulate the downcomer region below the cold leg in the late reflood phase of a postulated LBLOCA, in which the ECC injection from the SIT is terminated. During this period, most of the parameters in the primary system such as the system pressure, fluid temperature, ECC injection flow rate, reflood flow rate, and the heat flow rate from the downcomer wall to the fluids reach quasi-steady-state conditions, and hence the DOBO facility is designed for a steady-state operation.

Scaling Approach

The design of the DOBO facility was essentially based on the volume scaling law [10], which preserves the pressure, temperature, and elevation. In the standard volume scaling law, the length scale in the lateral direction is determined by the square root of the scaled area ratio. However, the size of the downcomer gap in the DOBO facility is kept at that of the APR1400, whereas the circumferential length of the downcomer wall is reduced 47.08-fold. It should be noted that information on the multidimensional phenomena in the lateral direction can be lost when using the volume scaling law because it is derived by using governing equations that assume a one-dimensional vertical flow [10]. However, the present scaling law overcomes this disadvantage because one of the two lateral coordinates was considered.

The approach of the present scaling law includes certain characteristics of the volume scaling law, such as a preservation of the velocity scale, heat flux, and hydrostatic head of the water column. In addition to these, the present scaling makes it possible to preserve some important local phenomena such as the axial void-fraction distribution, the thickness of the bubbly boundary, and the degree of a subcooling of the water.

However, the design of the DVI nozzle and its location does not follow the scaling law because it was found that the ECC water injected via DVI nozzles falls down along the core barrel wall in the form of a liquid film [2]. Therefore, its design is focused on a regeneration of the water film along the wall. For this, the diameter of the DVI nozzle of the DOBO facility was enlarged when compared to the 47.08-fold reduction for the APR1400, and it is intruded into the test section.

The major scaling ratios of the DOBO facility are summarized in Table I, and the detailed geometrical design of the test section is compared with that of the APR1400 in Fig. 2.

Table 1. Scaling Ratio of the DOBO Facility

Parameter	Scaling Law	
	Scaling Ratio	DOBO
Elevation	1	1
Gap Size Ratio	1	1
Width Ratio	l_R	1/47.08
Area Ratio	a_R	1/47.08
Volume Ratio	a_R	1/47.08
Velocity Ratio	1	1
Flow Rate Ratio	a_R	1/47.08
Gravity Ratio	1	1
Pressure Ratio	1	1
Temperature Ratio	1	1

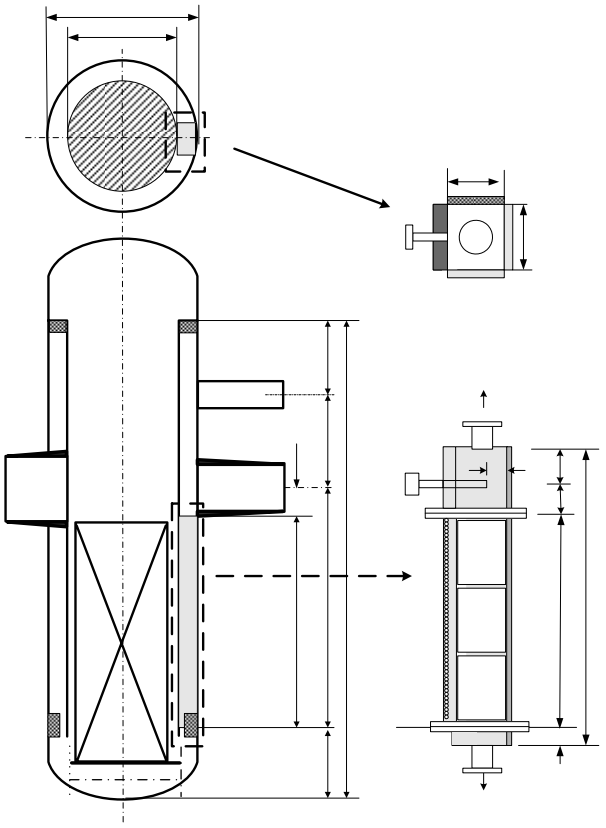

Fig. 2. Geometrical comparison of the reactor downcomer of the APR1400 and the test section of the DOBO facility

Fluid System

The DOBO facility consists of a test section, a steam–water separator, a condenser, a heat exchanger, a drain pump, a storage tank, an air injection and ventilation system, a preheater, a circulating pump, and an accumulator, as shown in Fig. 3. The maximum operation pressure is 500 kPa.

The test section is designed with a slab geometry which simulates the high-temperature wall of a reactor vessel from the cold leg to the flow skirt. However, its length was extended by 1.3 m to allow for an installation of a single DVI nozzle at the top of the test section and to drain the water at the bottom – but there is no heat input to this region. The width, depth, and total height of the test section are 0.3, 0.25, and 6.4 m, respectively. Only one of the four side walls (which has a length of 5.1 m) simulates a high-temperature reactor vessel wall, and thus the heat transfer area becomes 1.53 m^2.

The heat is generated by 207 cartridge heaters inserted in the wall. The maximum available heat flux is 100 kW/m^2, which corresponds to the maximum value at the termination of an ECC injection flow from the SIT, and this is controlled by a scilicon-controlled rectifier unit. Glass is installed on the adjacent and opposite walls of the heated wall to allow for a visual observation. The separator is connected to the outlet pipe of the test section for a phase separation of the two-phase flow. The separated water and steam phases are respectively cooled and condensed by two heat exchangers. The temperature of the water in the storage tank is controlled by the heat removal rates of the heat exchangers. The circulating water is injected into the test section at the top and drained at the bottom of the test section by two centrifugal pumps. The mass flow rate required for the DOBO facility during the reflood phase after emptying the SIT tanks is 1.3–1.4 kg/s. The circulating water mass flow rate of the test facility is maximally 3.3 kg/s and it is controlled by a control valve. The water level in the test section can be maintained at a fixed value by controlling the drain flow rate at the bottom of the test section. The water can be heated by up to 7°C at the maximum designed flow rate. The temperature of the ECC water injected via the DVI nozzle can be maintained at a target value by controlling the temperature of the accumulated water in the storage tank and the applied heat of the preheater. The system pressure is controlled by a piston-type accumulator (for fine control) and an air injection and venting system (for wide-range adjustment).

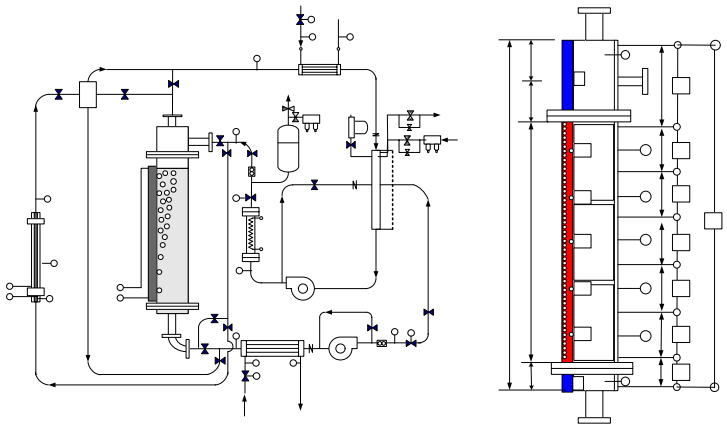

Fig. 3. Schematics of the Fluid System and the Location of the Instrumentations of the DOBO Facility

Instrumentations

Several kinds of commercial available instruments are installed for the boundary mass and energy flow rates. The location of each instrumentation is shown in Fig.3. The mass flow rates of the circulating water are measured by two Coriolis meters installed at the inlet and outlet pipes. The estimated uncertainty in a measured mass flow reading is 0.3%. The system pressure is measured at the top and bottom of the test section by two SMART-type pressure transmitters with an uncertainty estimated at 0.1%. Seven SMART-type DP (differential pressure) transmitters (LT-1 to LT-7) are uniformly spaced along the two pressure impulse taps of the pressure transmitters for measuring both the water level and the axial void fraction. An additional wide-range DP (LT-8) is installed to check the measured DP of the seven DP transmitters and the water level at the downcomer. The estimated uncertainty of each DP reading is 0.1%. The fluid temperatures are measured by several K-type thermo-couples, with uncertainties estimated as 2.2°C. These are installed at the inlet and outlet pipes, center of each DP taps, and also at the top and bottom of the test section. The surface temperature of a heated wall(TW) is also measured by thermocouples as shown in Fig.3. The applied power for the wall heating is measured by a power meter, with a reading uncertainty of 0.35%.

In addition to the above commercially available instruments, specially developed local 5-conductance probes are also installed for a measurement of the bubble parameters such as the void fraction and bubble velocity. The detailed locations of the local probes are also shown in Fig.3. Total five sensors are configured in a probe in order to investigate the multi-dimensional bubble behavior in a highly swirling two phase flow. For the benchmark of a local void fraction and bubble velocity, a separate test was performed in the air-water flow condition. The uncertainty of the void fraction is found to be 6.1% from the test[11].(Euh et al., 2005) The bubble velocity is measured by the signals from the two-sensors located at the up- and downstream for the configuration of the sensors. It is benchmarked with a photographic method by using a high speed camera in the separated test and the deviation is 3.01%. The traversing unit moves the probe in a two-dimensional direction by controlling the radial and rotational components. The probes are installed axially at five elevations of the test section to investigate the propagation of the local two-phase flow parameters.

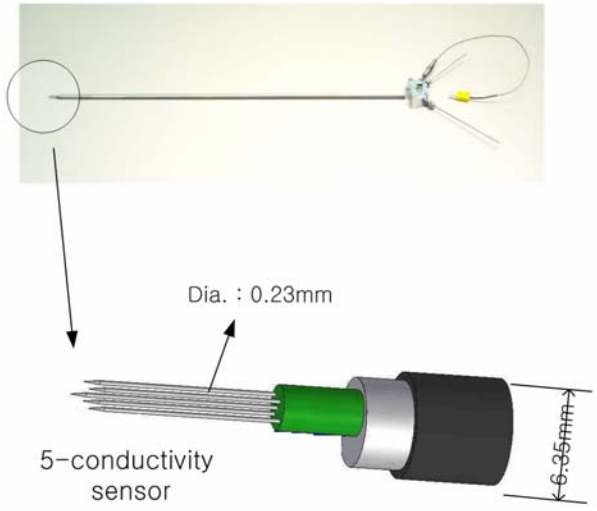

Fig. 4. Local 5-conductance probe

Experimental Condition and Procedure

The experimental condition was obtained by applying the scaling ratios in Table I to the RELAP5 results [5]. A single failure of a safety injection system was assumed in the RELAP5 calculation, and thus two of the four HPSIs (high pressure safety injections) were working. The test was performed from the condition at 250 s after the initiation of a LBLOCA, because the analysis results from RELAP5 showed that a downcomer boiling occurs during this time period. The reflood flow rate of the APR1400 was estimated at about 62.5 kg/s from RELAP5, and thus 1.33 kg/s of the ECC water should be delivered to the test section by the scaling law. During this period, the system pressure at the top of the test section changed from 170 to 160 kPa. In the test, the ECC water injected via a DVI nozzle into the test section simulates the penetrating water from the cold-leg level to the lower downcomer region in the APR1400. Therefore, the temperature of the injected ECC water was maintained the same as that of the water, where a mixture level exists, in the downcomer of the APR1400. RELAP5 estimated that the degree of a subcooling of the penetrated ECC water at this point was 15^{o}C at 250 s, and it decreased by up to 3^{o}C at the end of a LBLOCA. At this time, the heat flux of the downcomer wall of the APR1400 changed from 75 to 50 kW/m^2. In the test, the heat flux was changed to cover this range.

The test was started by injecting heated ECC water via a single DVI nozzle located at the top of the test section. The water mixture level was maintained above the top of the heated wall in the test section. Data acquisition began after all of the parameters had reached a steady state.

Experiments and Results

A total of five tests were performed in the reflood flow condition, according to the test conditions summarized in Table 2. However, the actual mass flow rate of the R1-R4 tests was 10% lower than the ideally scaled one. The R2-1 is a test to measure the local two phase parameters, of which the general thermal hydraulic conditions are similar to the R2.

Visual Observation

In the test, ECC water was delivered from the top of the test section and drained at the bottom. It should be noted that a bubble generated by the heated wall flows upward, and thus countercurrent flows of the steam and water phases are expected. Fig. 4 shows photographs taken through the transparent windows adjacent to the heated wall, which indicate a distinct bubble boundary layer (a typical characteristic of the subcooled boiling flow) occurring in the lower and middle regions of the test section, whose thickness changed with the heat flux. It is also evident from the photographs that the bulk-boiling region observed in the upper region of the test section is dramatically expanded as the applied heat flux is increased. The findings from the visual observation can be summarized as follows:

Table 2. Summary of the Experimental Conditions

Parameter	T_{ECC} (^{o}C)	P_{sys}(kPa)	W_{ECC}(kg/s)	$q"$(kW/m^2)
R1	110.1	162.8	1.22	50.2
R2	110.2	161.4	1.16	69.7
R3	109.6	166.5	1.20	82.1
R4	109.5	170.8	1.20	91.1
R2-1	110.7	158.5	1.33	70.5

The void fraction decreased as the elevation decreased. This is expected because the degree of a subcooling of the injected ECC water at the top of the test section was small and the heat transfer from

the heated wall to the ECC water did not exceed the increase of a subcooling resulting from the hydrostatic head at the bottom of the test section. In the present test, the increase in the pressure difference at the bottom resulting from the accumulated water was 40 kPa, and it caused an increase of the subcooling by 6.7°C.

The photographs in Fig. 5 show a typical characteristic of a subcooled boiling flow. In the lower region of the test section, the average void fraction was negligible. The onset of a nucleate boiling (ONV point) occurred in this region, and the generated bubbles remained on the heated wall until their diameter increased to a few millimeters, at which point they were detached from the wall. The detached bubbles slid along the wall, and thus the thickness of the bubbly boundary layer gradually increased. Downstream of this region, the void fraction and the thickness of the bubbly boundary layer began to increase rapidly, which is the point of an onset of a void where a significant void fraction developed.

In the middle region of the test section, cap shaped bubbles generated by the coalescence of small bubbles were accompanied with small bubbles even though the void fraction was less than a few percent, and these slid up the wall. The bubble boundary layer thickened rapidly as it traveled upward, with the thickness changed due to a periodic swirling motion of the bubble clusters comprising of groups of small bubbles. The swirling motion from the heated wall to the cold-water core region was due to an unbalanced distribution of the velocities of the two phases between the inside and outside of the bubble boundary layer. The velocities of the two phases increased due to an increase of the local void fraction inside the bubble boundary layer, and this also caused an increase in the velocity of the downward liquid flow in the water core region. This phenomenon resulted in a lateral motion of the bubble clusters. Small amounts of stagnant or flowing-downward bubbles were also observed periodically in the water core region. The swirling motion of the high-temperature bubble clusters can enhance the interfacial heat transfer between the two phases.

Well-mixed bulk boiling occurred in the upper region that expanded toward the middle and bottom regions as the heat flux increased. The void fraction was in the range of 10–20%, and the observed flow regime was a churn-turbulent flow. Bubble breakup – rather than a bubble coalescence – was dominant in this highly turbulent region

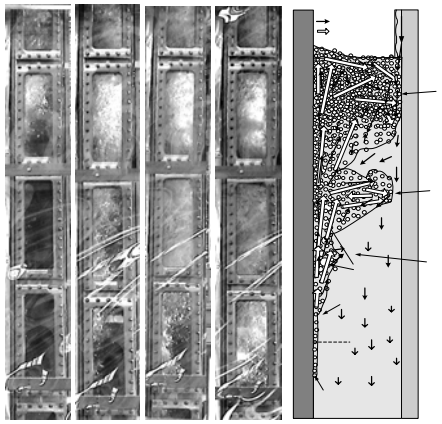

(a) R1 (b) R2 (c) R3 (d) R4 (e) Illustration

Fig. 5. Photograph and typical illustration of a downcomer boiling in the DOBO

Global Two-phase Flow Parameters

The average axial void-fraction distribution was measured in the present test by using DPs. Here, the void fraction, α, is obtained from the measured collapsed level according to

$$\alpha = 1 - \frac{h}{H} \tag{1}$$

where h and H are the measured collapsed level and the distance between the taps for the DP transmitters, respectively. Fig. 6 shows the axial distribution of the average void fraction according to the applied heat flux. The mixture level was maintained between the two pressure taps of LT-7, and thus the void fraction exceeded 0.4 at LT-7 for all the cases. The decrease in the void fraction of LT-7 with an increasing applied heat flux was due to the collapsed water level being controlled by a wide-range level transmitter LT-8, which covers from LT-1 to LT-7. As shown in Fig. 6, the void fraction was negligible below an elevation of 2.8 m, but it was significant above it for all the cases. This indicates that an increased heat flux resulted in an increase in the void fraction above 2.8 m. The overall average void fraction of the heated region was less than 9% for a given maximum heat flux condition. This low void fraction is somewhat different from the result from the best-estimate code (e.g., the void fraction from the RELAP5 calculation was more than 40%, even in the middle region) [5]. The 9% void fraction resulted in a 9% reduction of the collapsed level and then a 3% decrease in the reflood flow rate if no other parameters were not changed by the boiling. The present data implies that a degradation of the hydrostatic head for a core reflooding is not especially significant, and that the thermal hydraulic models of the RELAP5 code related to a downcomer boiling should be improved.

Fig. 7 shows the degree of a subcooling of the fluid at the bottom of the test section. In the test, the subcooling of the temperature of the injected ECC water was 2.5°C to 5.0°C, which is slightly higher than that of the APR1400. The figure also clearly shows that the ECC water did not reach the saturated temperature and that the degree of a liquid subcooling at the bottom of the test section was maintained in the range 4.3–5.5°C. It should be noted that the temperatures of the injected ECC water for the R3 and R4 tests were higher than those for R1 and R2, which must have affected the degree of a subcooling at the bottom.

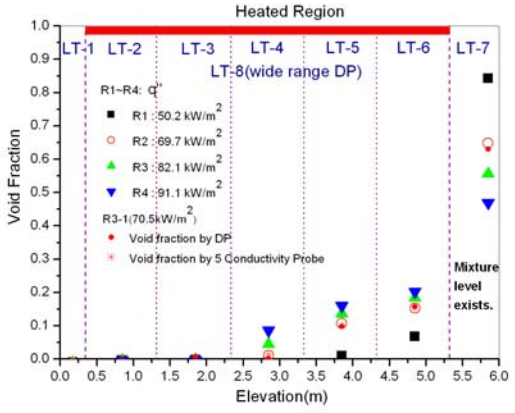

Fig. 6. Axial void fraction distribution

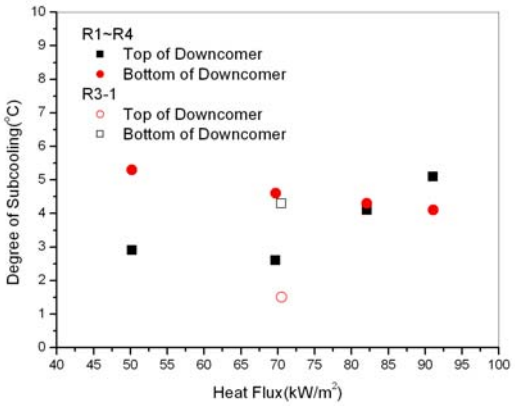

Fig. 7. Degree of a subcooling of the fluid

Local Two-phase Flow Parameters

The local bubble parameters were measured by 5-conductance probes at 70.5kW/m^2 of a heat flux condition which corresponds to the R2-1 of Table 2. The experimental condition was similar to that of the R2 case of Phase-I, however, it should be noted that the injection flow rate via a DVI nozzle was increased by about 10% when compared to the R2, which is a closer initial condition to the safety analysis code results. A total of five planes were selected for the local measurements along the heated test section and each measuring plane was located at the midpoint between each DP tab. On the measuring plane, six measuring paths perpendicular to the heated wall were chosen. Among them, five were located on a half of the measuring plane and one was located on the other half of the plane to check for a symmetry of the obtained data (see the Fig.8). The data was acquired at 25 points along each measuring path and the acquired time was 30 seconds at each point.

Fig. 10 shows the local void fraction profiles at each elevation of the test section. At the lower part where the boiling is initiated, steam is concentrated near the wall. As the generated steam flows upward, the void profile became wide and a distinct bubbly boundary layer was found. However, at the two highest regions, a center peaking of the void profile was observed. This trend coincided well with the visual observation that the bubbly boundary layer thickness increased rapidly as the elevation became higher. The void fraction distributions at the lower three elevations showed that the local void fraction adjacent the side wall was higher than that of the center line. It must be due to the wall effect. In the near side wall of the rectangular channel, the phasic velocity was lower than the center line due to an increased wall shear effect. The contour plot of the surface temperature of a heating wall confirms this fact well as shown in Fig. 9. The surface temperature of the heated wall increased as it moved toward the side wall due to a lower fluid velocity. The average void fraction can be obtained from the local void fraction distribution. Fig. 6 compares the average void fractions obtained from the local void fraction and the DPs. It shows that the present measurement method and the acquired data of the local void fraction are reliable even though they have a high uncertainty range. Actually, the high uncertainty of the measured local void fraction is mainly due to the oscillatory swirling behavior of the bubbles.

Fig. 11 shows the bubble velocity distribution and its contour plot. At the two highest elevations, the profile of the bubble velocity is similar to that of the void fraction. In the opposite side to the heated wall, the bubble velocity is very low or negative since the upward bubble motion is suppressed by the downward liquid. The bubble velocity near the side wall is small when compared to that of the center line as stated above.

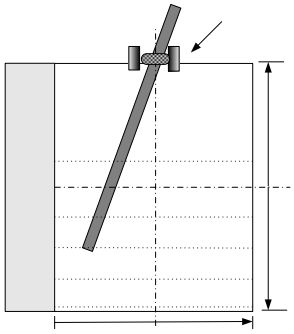

Fig. 8. Measurement points for the local bubble parameters

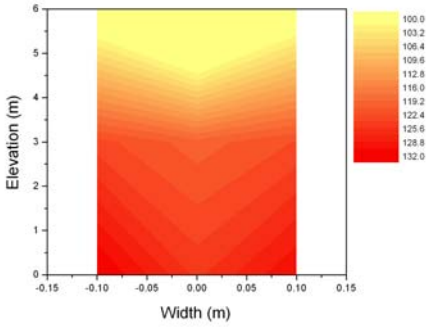

Fig. 9. Contour of surface temperature on the heated wall(R2-1)

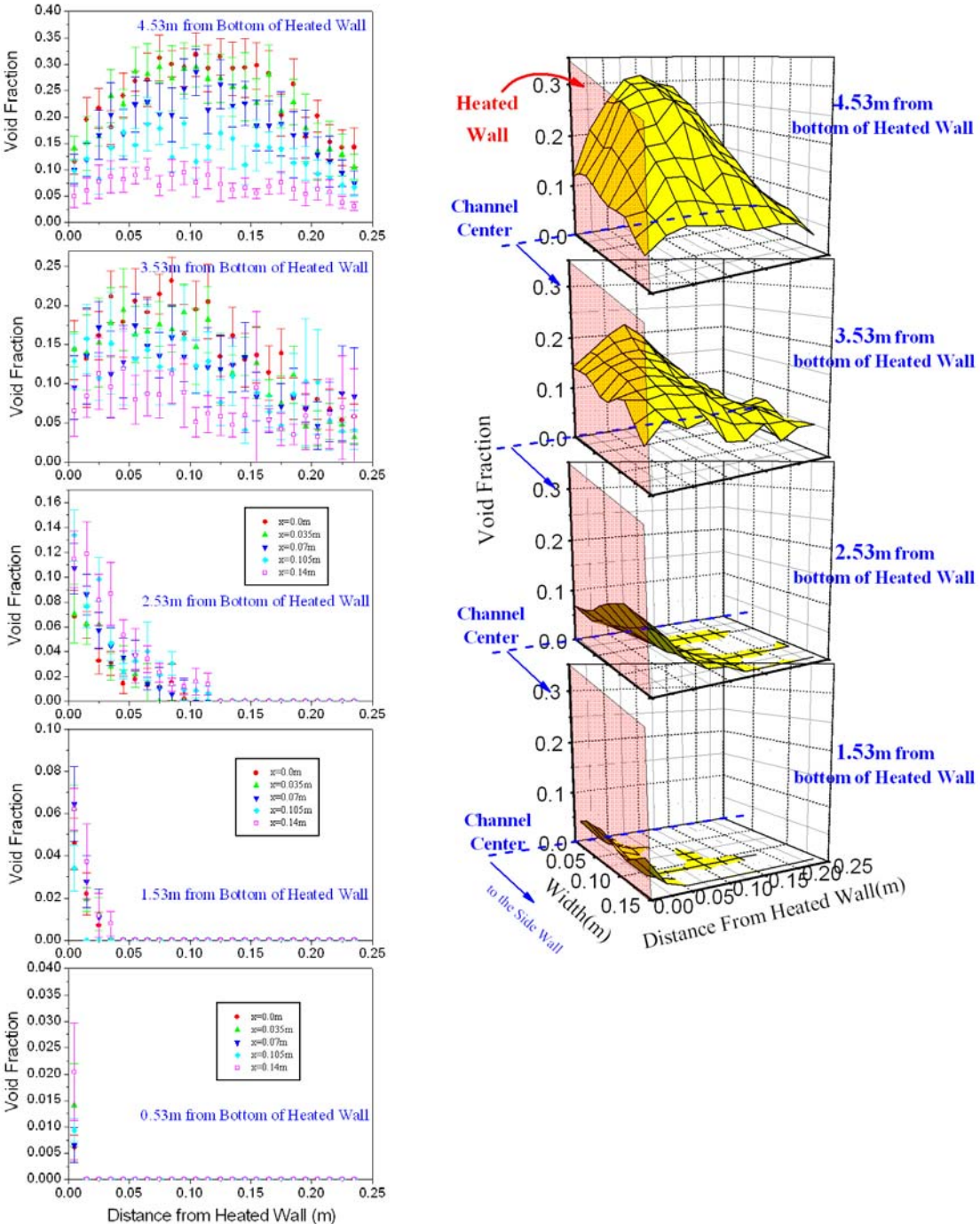

Fig. 10.Local void fraction distribution and contour plot(R2-1)

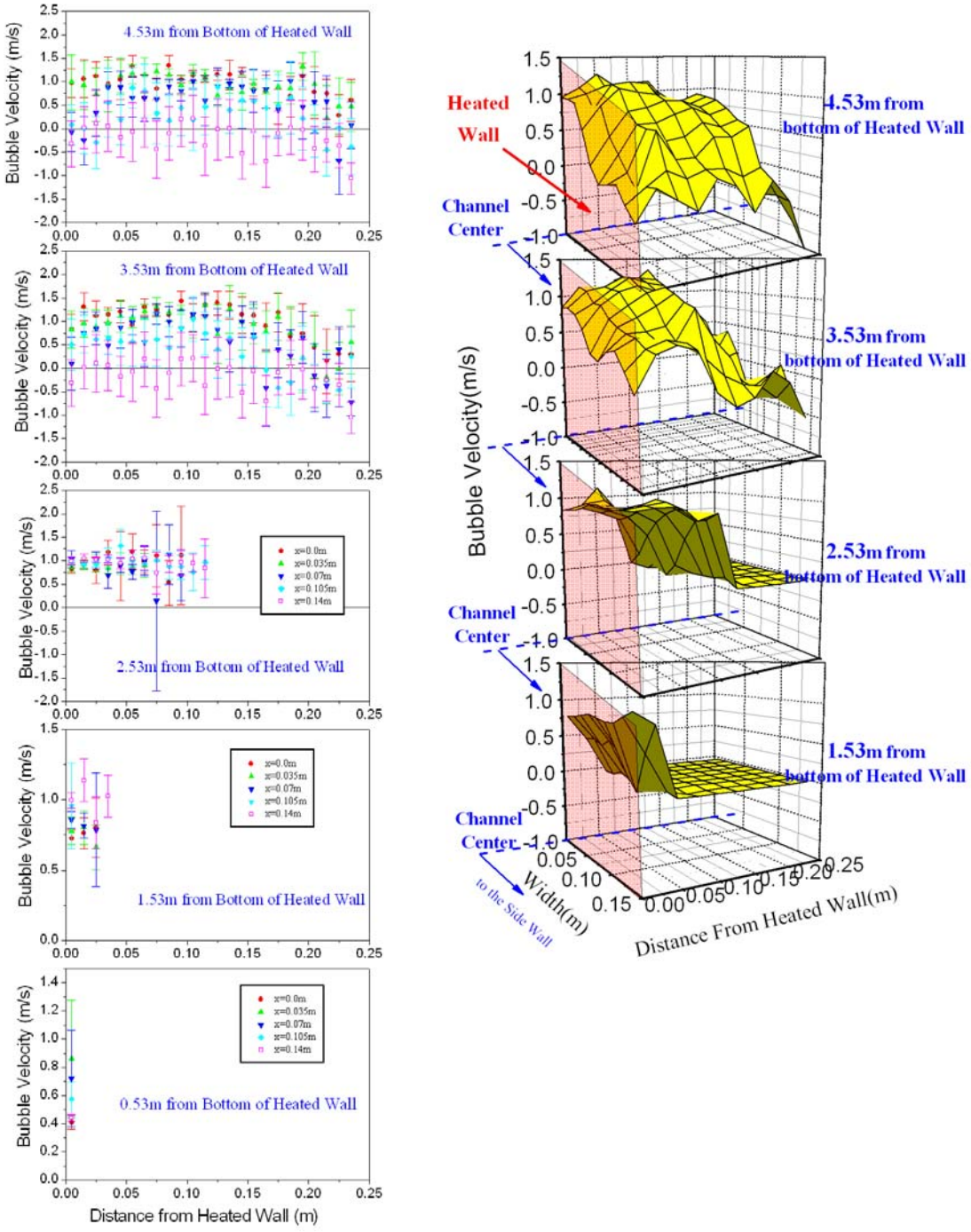

Fig. 11. Local bubble velocity distribution and contour plot(R2-1)

Conclusion

For an investigation of the downcomer boiling phenomena experimentally, a separate effect test was performed in the DOBO facility. Observation of the test revealed the occurrence of a countercurrent subcooled boiling flow, and the creation of a distinct bubble boundary layer whose thickness varied dramatically with the applied heat flux. The data showed that the channel average void fraction was small at the anticipated heat flux condition of the reflood period of a LBLOCA , and thus the reduction of the hydraulic head for the core reflood was not too severe in the present test condition, with a subcooling margin of 4.3–5.5^{o}C at the bottom of the test section. For the quantification of a multidimensional flow, the local two-phase parameters such as bubble velocity of each phase and void fraction were also measured by using a newly designed local 5-conductance probe. The local distributions of various parameters reflected well the results from the visualization. The generated experimental data will be utilized to enhance a code's capability for the multi-dimensional two-phase flow shown in the downcomer boiling test.

In further studies, the three dimensional local bubble velocity, local interfacial area concentration and local bubble distributions will be obtained from the acquired data of the 5-conductance probes. In addition, the local liquid velocity and the local fluid temperature will be measured by a specially designed instrumentation spool piece consisting of a local bi-directional flow tube and a thermocouple.

ACKNOWLEDGEMENTS

The authors wish to express their deep appreciation to Mr. W.M.Park and Dr. H.K.Cho at KAERI and Mr. B.U.Bae at Seoul National University for their assistance of the experimental work. This study has been carried out under the nuclear R&D program by the Korean Ministry of Science and Technology

REFERENCES

1. S.J.CHO, B.S.KIM, M.G.KANG and H.G.KIM, "The Development of Passive Design Features for the Korean Next Generation Reactor," Nucl. Eng. Design, **201**, 259 (2002).
2. B.J.YUN, T.S.KWON, W.M.PARK, J.K.PARK, C.-H.SONG, D.J.EUH and I.C. CHU, "Direct ECC Bypass Phenomena in the MIDAS Test Facility during LBLOCA Reflood Phase, " Journal of the KNS, **34**, 5 (2002).
3. B.J.YUN, H.K.CHO, D.J.EUH, C.-H.SONG and G.C.PARK, "Scaling for the ECC Bypass Phenomena during the LBLOCA Reflood Phase, " Nucl. Eng. Design, **231**, 315 (2004).
4. T.S.KWON, B.J.YUN, D.J.EUH, I.C. CHU and C.-H.SONG, "Multidimensional Mixing Behavior of Steam-water flow in a Downcomer Wnnulus during LBLOCA Reflood Phase with a Direct Vessel Injection Mode, " Nuclear Technology, **143**, 1 (2003).
5. S. W. Lee and S.J.Oh, "Experimental Benchmarking and Safety Analyses of APR1400 Large Break LOCA Scenario", Proc. 5th Int. Congress on Advances in Nuclear Power Plants(ICAPP05), Seoul, Korea, May 15-19 (2005).
6. B.D.CHUNG, Y.J.LEE. C.-H.SONG, T.S.KWON, S.M.LEE and I.G.KIM, "Development of Interfacial Drag for Bubbly Flow in Downcomer during Reflood Phase of APR1400 LBLOCA," Proc. 2004 KNS Autumn Meeting, Yongpyong, Korea, October 28-29, Korea Nuclear Society (2004) (CD-ROM).

7. S.W.LEE, H.G.KIM and S.J. OH, "The Post-Test Analyses of CCTF C2-4 using TRAC-M and RELAP Codes," Proc. 3rd Korea-Japan Symposium on Nuclear Thermal Hydraulics and Safety(NTHAS3), Kyeongju, Korea, October 13-16 (2002B).
8. Y. SUDO and H.AKIMOTO, "Downcomer Effective Water Head during Reflood in Postulated PWR LOCA," Journal of Nuclear Science and Technology, **9**,1 (1982).
9. B.J.YUN, D.J.EUH and C.-H. SONG, "Investigation of the Downcomer Boiling Phenomena During the Reflood Phase of a Postulated Large-Break LOCA in the APR1400," to be published in the Nuclear Technology, October (2006)
10. A.N.NAHAVANDI, F.S.CASTELLANA and E.N.MORADKHANIAN, "Scaling Laws for Modeling Nuclear Reactor Systems, " Nucl. Sci. & Eng., **72**, 75 (1979).
11. D.J.Euh, B.J.Yun, W.M.Park and C.-H Song, "Investigation of the Transport of the Bubble Parameters in Air/Water Flow Conditions", ICAPP05, Seoul, Korea (2005)